

## The Influence of Aluminum Oxide Nanoparticles on the Characterizations and Mechanical Performance of Epoxy Matrix Composite



Qusay H. Mohammed<sup>\*</sup>, Abdulhaqq A. Hamid<sup></sup>

Department of Mechanical Engineering, College of Engineering, University of Mosul, Mosul 41002, Iraq

Corresponding Author Email: [qusay.24enp42@student.uomosul.edu.iq](mailto:qusay.24enp42@student.uomosul.edu.iq)

Copyright: ©2026 The authors. This article is published by IETA and is licensed under the CC BY 4.0 license (<http://creativecommons.org/licenses/by/4.0/>).

<https://doi.org/10.18280/rcma.360213>

### ABSTRACT

**Received:** 30 January 2026

**Revised:** 18 March 2026

**Accepted:** 27 March 2026

**Available online:** 30 April 2026

#### Keywords:

*Al<sub>2</sub>O<sub>3</sub>, epoxy resin, mechanical properties, nanocomposites, nanoparticles*

The mechanical performance of epoxy/Al<sub>2</sub>O<sub>3</sub> nanocomposites was significantly improved in this work, without compromising structural rigidity. The main objective of this work was to determine the optimum nanoparticle concentration that achieved a balance between reinforcement and dispersion quality, and to overcome the brittleness of epoxy resins. Nanocomposites with different alumina weight percentages (1, 2, 4, and 6 wt.%) were fabricated by utilizing mechanical stirring and ultrasonic dispersion to guarantee homogeneous particle distribution. Tensile, impact, flexural, and hardness tests were performed for the mechanical examination process, and Fourier Transform Infrared (FTIR) spectroscopy and scanning electron microscopy (SEM) were used to characterize the nanocomposites. The findings indicated that the maximum increases in tensile and flexural strengths were 41.73% and 12%, respectively, at 2 wt.% of Al<sub>2</sub>O<sub>3</sub>, while the maximum improvements in toughness and hardness were 38.64% and 28%, respectively, at 6 wt.% of Al<sub>2</sub>O<sub>3</sub>, compared to pure epoxy resin. SEM analysis confirmed that the optimized processing method decreased agglomeration, which otherwise reduced performance at higher loadings (6 wt.%). This improved technique provides a scalable and efficient method for creating toughened polymer matrices, with important effects for structural design and superior coatings in automotive and aerospace applications.

## 1. INTRODUCTION

Epoxy resin matrix composites have been extensively used in the automobile, construction, electronics, and aerospace industries due to their excellent mechanical and thermal properties [1]. Epoxy is one of the most popular thermosetting polymers, which, after curing, forms a three-dimensional crosslinked network [2]. Because of these properties, it is used as a matrix for the production of polymer composites [1].

However, these advantages come with certain disadvantages in the mechanical properties of epoxy resin, such as low fracture toughness, low tensile strength, and brittleness, which lead to poor resistance to crack formation and propagation [3]. These limitations prohibit the use of these polymers in high-performance applications requiring mechanical strength. Expanding the range of polymer applications requires improving mechanical properties, as the materials must withstand heavy loads and challenging environmental conditions [4].

One way to address these limitations is to use various filler and reinforcing materials to enhance the properties and decrease the brittleness of cured epoxy. Therefore, recent research on epoxy polymers primarily focuses on applications employing particle reinforcement [5].

The use of particulate fillers produces consistent mechanical properties in every direction [6]. Particulate fillers include

metals [7], metal oxides [8], natural rubber [9], and ceramics [10]. The dimensions of the filler particles range from microscale to nanoscale [11]. Nanoscale measures less than 100 nm in at least one dimension [12].

Significant enhancements in epoxy polymer properties have been obtained by utilizing nano-sized particles compared to micro-sized ones [5]. The incorporation of nanoparticles as a reinforcement, which presents a high surface area to volume ratio, greatly improves the interaction between the matrix and the nanoparticles [13].

Improving mechanical properties requires a high level of interfacial bonding between the polymer and nanoparticles. Due to the high viscosity of polymers and the cohesiveness that causes agglomeration, it can be difficult to disperse nanoparticles uniformly. Therefore, researchers generally need a method to ensure homogeneous distribution in a highly viscous liquid [14].

Numerous dispersion techniques have been used to combine polymers and nanoparticles, including ball milling, high shearing mixing, and ultrasonication [15]. The latter technique is very effective in achieving a homogeneous dispersion [16].

In this method, high-intensity ultrasound waves are introduced into the mixture to form cavitation bubbles. These bubbles begin to grow until they reach a specific diameter and then collapse. This collapse creates a hot zone with extremely high local temperature and pressure. These hot zones may

subsequently cause the disintegration of nanoparticle aggregates in the mixture [17].

Nano- $\text{Al}_2\text{O}_3$  represents one of the most extensively utilized metal oxides for manufacturing polymer nanocomposites because of its exceptional mechanical properties, high hardness, and chemical and thermal stability, as well as reduced cost of  $\text{Al}_2\text{O}_3$  nanoparticles compared to nanofillers made from carbon and nano- $\text{TiO}_2$  [18].

Many studies have focused intensively on this field; initially, Wu et al. [19] used epoxy resin as a matrix reinforced with 30 nm  $\text{Al}_2\text{O}_3$  nanoparticles at various concentrations (1, 3, 5, and 7 wt.%). The mixture was mixed mechanically. Mechanical tests, including impact and tensile tests, were carried out on the samples. The findings showed a significant enhancement in the mechanical properties of the nanocomposites, with tensile strength increasing by 82.60% and impact strength by 63.58% compared to pure epoxy at a concentration of 3 wt.% of  $\text{Al}_2\text{O}_3$ .

Recent investigations by Zhang et al. [20] have used silane coupling compounds KH550, KH560, and KH570 to modify the surface of alumina nanoparticles before manufacturing epoxy nanocomposites. Mechanical properties, like hardness and tensile strength, have been evaluated. The findings demonstrated that the KH570-treated composite materials showed significant improvements in tensile strength (49.1%) and hardness (8.8%). These findings show that surface-modified  $\text{Al}_2\text{O}_3$  nanoparticles may be used as reinforcements in epoxy composites efficiently and effectively.

There is a knowledge gap regarding the ideal balance of mechanical performance in nanocomposites for construction applications since using alumina nanoparticles to achieve significant enhancements in mechanical properties demands exact control in weight ratios and dispersion techniques.

Therefore, the primary objective of this research is to improve the mechanical properties of epoxy resin by adding  $\text{Al}_2\text{O}_3$  nanoparticles; optimize the ratio of reinforcement that maximizes improvement and minimizes particle aggregation; evaluate hardness, flexural, impact, and tensile properties; and examine the morphological properties and particle distribution by using scanning electron microscopy (SEM).

## 2. EXPERIMENTAL DETAILS

### 2.1 Materials

The epoxy used as the matrix material in this work was Sikadur<sup>®</sup> 52 LP, provided by the Swiss Company (Sika); it consists of two parts: part A (epoxy resin) and part B (hardener), and it is chemically classified under the epoxide

family and is referred to as Diglycidyl Ether Bisphenol-A (DGEBA).

It also has good properties at high temperatures, is solvent-free, has low viscosity, demonstrates shrinkage-free curing, and has high mechanical and adhesive strength.

Nano- $\text{Al}_2\text{O}_3$  used in this study was in the form of a white powder nanoparticle, alpha phase, 99.9% purity, an average particle size of 50 nm, and provided by Skyspring Nanomaterials USA Company. Many characteristics of both materials are shown in Table 1.

**Table 1.** Material characteristics according to the manufacturer's specifications

Property	Epoxy	$\text{Al}_2\text{O}_3$
Density	1.06 g/cm <sup>3</sup>	3.9 g/cm <sup>3</sup>
Appearance	Transparent	White
Type	DGEBA	Alpha
Mixing ratio resin: hardener	2:1	
Size		50 nm
Viscosity	330 mPa.s at 25 °C	
Company	Sika	Skyspring

### 2.2 Method of nanocomposites preparation

The epoxy was reinforced with different concentrations (1, 2, 4, and 6 wt.%) of  $\text{Al}_2\text{O}_3$  nanoparticles. These concentrations were chosen based on initial experiments and published studies on epoxy nanocomposites.

Previous research by Wu et al. [19] has shown that adding nanoparticles within the ratios (1, 3, 5, and 7 wt.%) significantly improves mechanical properties and identifies the agglomeration levels.

In our study, concentrations higher than 6 wt.% were avoided because they increase the viscosity of the epoxy, making nanoparticle dispersion difficult and initiating aggregation.

Initially, the nanoparticles were mixed with the epoxy mechanically at the specified ratios using a low-speed mixer for 10 minutes to ensure a uniform mixture between the matrix and the reinforcement. This was followed by ultrasonication using an ultrasonic probe for 30 minutes at an amplitude of 60% of the maximum power, as per the research by Kumar et al. [21].

Ice is added around the beaker so that the temperature of the epoxy does not rise. Finally, the hardener is added to the mixture and mechanically mixed for 5 minutes at a slow speed to reduce the creation of air bubbles.



(1) Adding epoxy



(2) Weighting nanoparticles



(3) Adding nanoparticles to epoxy

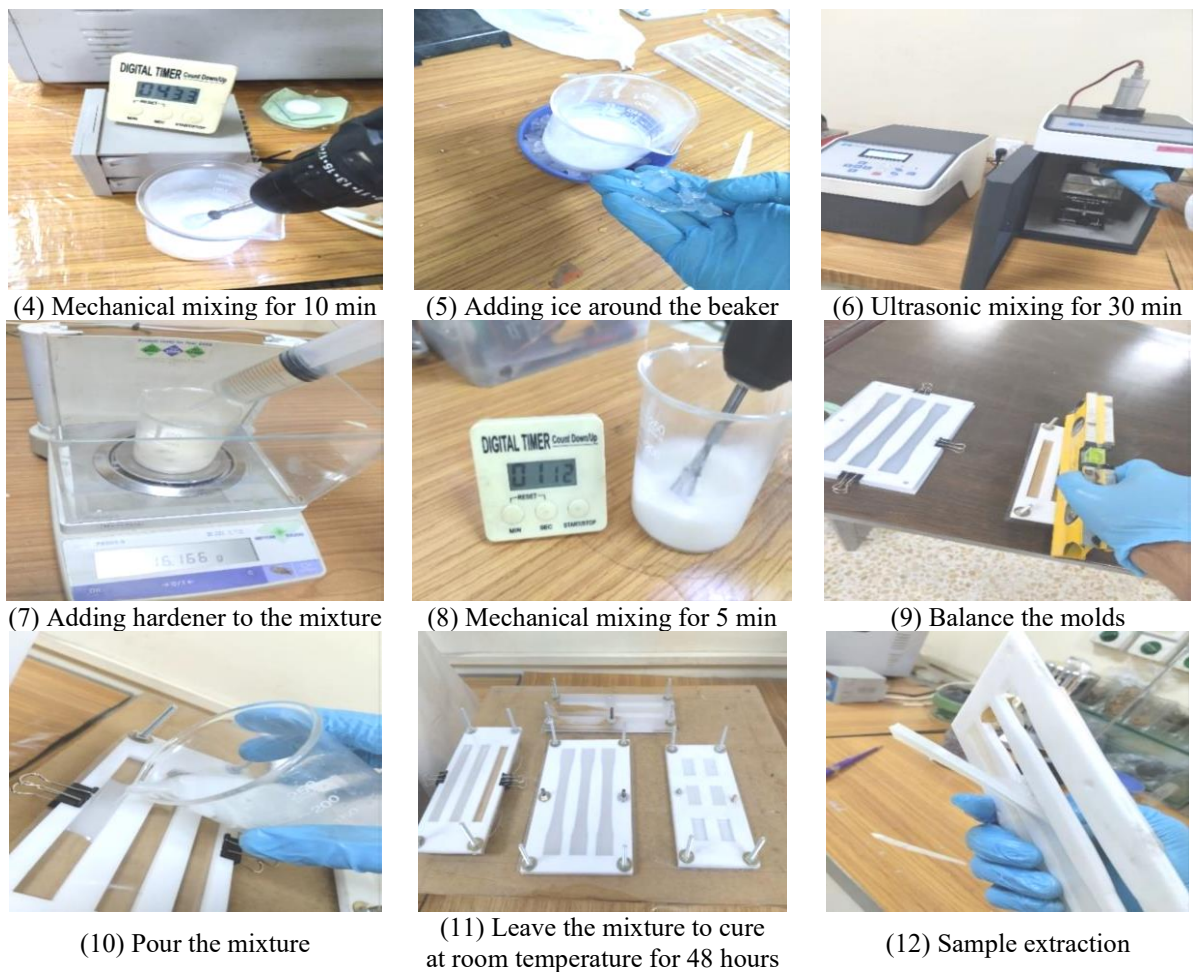


**Figure 1.** The different steps for preparing nanocomposites

After completing the mixing process, Vaseline was applied to the casting molds before pouring the mixture to prevent the epoxy from sticking to the molds; then the mixture was poured into molds and left to cure at room temperature (25 °C) for 48 hours.

Three samples were taken and tested for each examination, and then their averages were recorded. All molds were manufactured locally from acrylic material according to international standards (ASTM). Figure 1 shows the different steps for preparing nanocomposites.

### 3. MECHANICAL TESTS

#### 3.1 Tensile test

The tensile strength of the sample was measured by a computerized universal testing machine, type (Yisite), model (EWN-20kN), with a crosshead speed of (5 mm/min) and a loading rate of 10 N/sec, as seen in Figure 2. The measurements of the tensile test specimen conform to ASTM D-638 [22] and are dog-bone shaped, as shown in Figure 3.

#### 3.2 Flexural test

The flexural test was performed according to the ASTM D-790 [22] standard by utilizing a universal testing machine type (ALFA) with a crosshead speed of (15 mm/min) and a capability of (20 kN), as shown in Figure 4. Flexural inspection of plastics and polymer composites is usually

performed using a three-point test. Three samples were taken for each case, tested, and their averages were reported (see Figure 5).



**Figure 2.** Computer-controlled tensile testing machine (Yisite)

#### 3.3 Impact test

This test measures a material's strength when exposed to a sudden force. The testing was conducted using a pendulum impact tester, Izod type, model BROOKS; see Figure 6. The dimensions of the impact test sample conform to ASTM E23 [23], as shown in Figure 7.



(a)



(b)

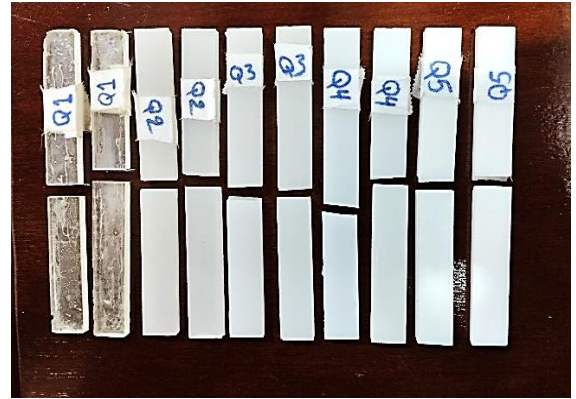
Figure 3. Samples of a tensile test: (a) before the test, (b) after the test



Figure 4. Flexural test device (ALFA)



(a)

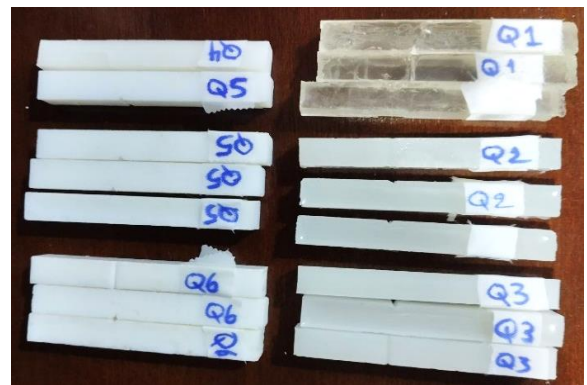


(b)

Figure 5. Samples of flexural test: (a) before the test, (b) after the test



Figure 6. Izod impact test device (Brooks)



(a)



(b)

Figure 7. Samples of impact test: (a) before the test, (b) after the test

### 3.4 Hardness test

Hardness is defined as the ability of a material to resist scratching or penetration. The test was carried out by utilizing a digital Shore D (Durometer), as illustrated in Figure 8. The dimensions of the hardness samples are according to ASTM D 2240 [22], as shown in Figure 9.



Figure 8. Shore D (Durometer) device



(a)



(b)

Figure 9. Samples of hardness test: (a) before the test, (b) after the test

## 4. CHARACTERIZATIONS

### 4.1 Scanning electron microscopy

The SEM is a crucial tool for visualizing materials at the micron level and, in some cases, even submicron resolution. With a maximum resolution of approximately 2.5 nanometers and a magnification of up to 300,000 times, the excellent resolution of the SEM is a key factor in its application. Furthermore, the three-dimensional appearance of the sample in SEM images is another advantage. Therefore, when other particles alter the surface of a sample, the SEM is highly effective in characterizing its crystalline, magnetic, and

electrical properties, as well as determining whether any changes in particle shape have occurred [24].

The device used in this study is of the type TESCAN, MIRA3, Czech Republic; see Figure 10. The SEM micrograph of an  $\text{Al}_2\text{O}_3$  nanoparticle is presented in Figure 11.



Figure 10. Scanning electron microscopy (SEM) device (TESCAN)

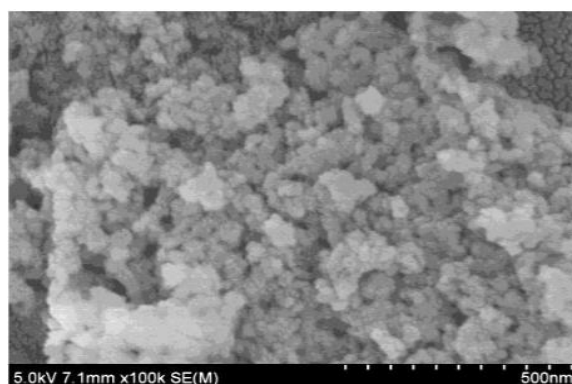


Figure 11. Scanning electron microscopy (SEM) micrograph of the as-received  $\text{Al}_2\text{O}_3$  nanoparticle

### 4.2 Fourier Transform Infrared spectroscopy

Fourier Transform Infrared (FTIR) analysis was used to study novel species and structural changes in functional groups on nanoparticles. This analysis allows for the determination of the vibrational properties of chemical functional groups in a sample.

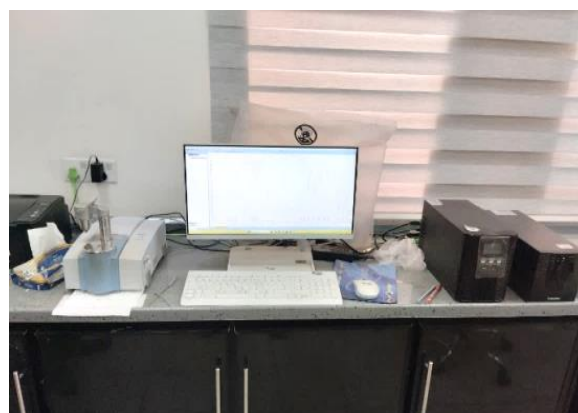


Figure 12. Fourier Transform Infrared (FTIR) spectroscopy device (BRUKER)

These groups absorb infrared radiation within a specific wavenumber range when interacting with the sample, due to the stretching, contraction, and twisting of intermolecular bonds.

FTIR analysis is used to record the transmittance versus wavenumber to characterize the absorption of the studied sample across different wavenumbers of infrared radiation [25]. Device used for inspection: BRUKER spectrometer, as shown in Figure 12.

## 5. RESULTS AND DISCUSSION

### 5.1 Tensile properties of Al<sub>2</sub>O<sub>3</sub>-epoxy nanocomposites

The tensile tests were conducted on epoxy and nanocomposites with various nanoparticle weight percentages of alumina. Figure 13 demonstrates a brittle behavior for all the stress-strain curves, and the tensile strength gradually increases with increasing alumina nanoparticle wt.% until it reaches its maximum increase of 41.73% at 2 wt.% Al<sub>2</sub>O<sub>3</sub> compared with pure epoxy, as illustrated in Table 2.

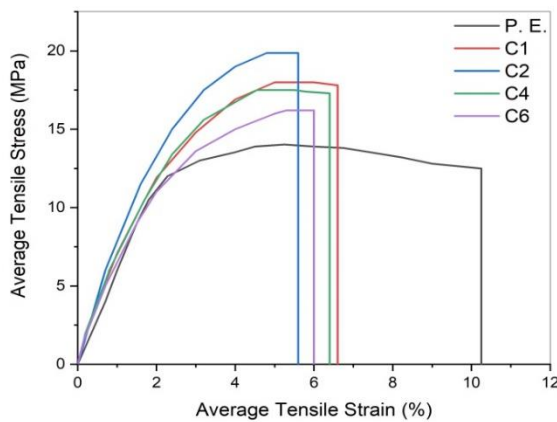


**Figure 13.** Stress-Strain curves of EP-Al<sub>2</sub>O<sub>3</sub> nanocomposites

Note: P.E.: Pure Epoxy, C1: Composite with 1 wt.% Al<sub>2</sub>O<sub>3</sub>, C2: Composite with 2 wt.% Al<sub>2</sub>O<sub>3</sub>, C4: Composite with 4 wt.% Al<sub>2</sub>O<sub>3</sub>, C6: Composite with 6 wt.% Al<sub>2</sub>O<sub>3</sub>

**Table 2.** Tensile test results of EP-Al<sub>2</sub>O<sub>3</sub> nanocomposites

Sample's Code	Composition	Ultimate Stress (MPa)	Strain at Break (%)
P.E.	Pure epoxy 99 wt. %	14.02	10.30
C1	epoxy + 1 wt. % Al <sub>2</sub> O <sub>3</sub> 98 wt. %	18.00	6.56
C2	epoxy + 2 wt. % Al <sub>2</sub> O <sub>3</sub> 96 wt. %	19.87	5.60
C4	epoxy + 4 wt. % Al <sub>2</sub> O <sub>3</sub> 94 wt. %	17.57	6.42
C6	epoxy + 6 wt. % Al <sub>2</sub> O <sub>3</sub>	16.21	6.00

This improvement is attributed to the uniform distribution of nanoparticles within the epoxy and the effective interfacial adhesion between the reinforcement and the matrix, which results in facilitating stress transfer between them.

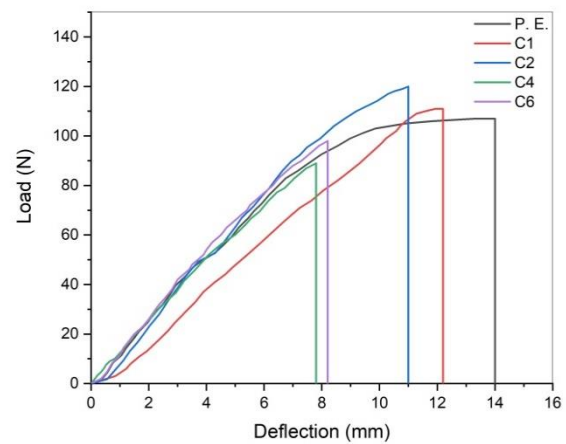
Our maximum increase in tensile strength is less than the 82.6% achieved by Wu et al. [19], because they used ultrasonic mixing for a longer period (about 4 hours), resulting in a better distribution of nanoparticles and a significant increase in tensile strength.

On the other hand, increasing the alumina content above 2 wt.% resulted in a gradual decrease in tensile strength, likely because of the agglomeration of nanoparticles within the epoxy, which increases stress concentration and subsequently leads to crack initiation and propagation. These results are consistent with the SEM images presented in the current study.

### 5.2 Flexural properties of Al<sub>2</sub>O<sub>3</sub>-epoxy nanocomposites

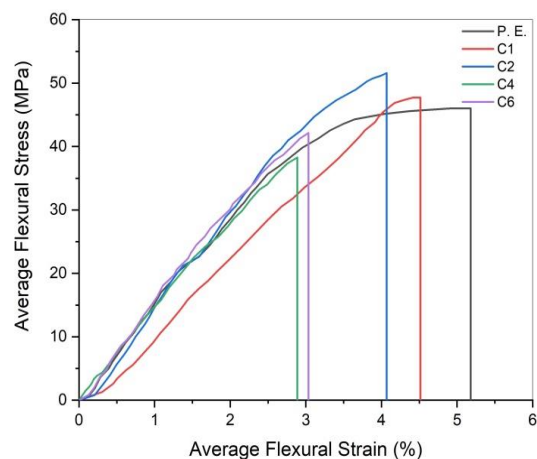
The flexural strength of nanocomposites was measured with different ratios of alumina nanoparticles. Figure 14 represents load-deflection curves of EP-Al<sub>2</sub>O<sub>3</sub> nanocomposites.

Figure 15 shows that the flexural strength increased gradually with increasing amounts of Al<sub>2</sub>O<sub>3</sub> up to 2 wt.%, then deteriorated beyond this percentage.



**Figure 14.** Load-Deflection curves of EP-Al<sub>2</sub>O<sub>3</sub> nanocomposites

Note: P.E.: Pure Epoxy, C1: Composite with 1 wt.% Al<sub>2</sub>O<sub>3</sub>, C2: Composite with 2 wt.% Al<sub>2</sub>O<sub>3</sub>, C4: Composite with 4 wt.% Al<sub>2</sub>O<sub>3</sub>, C6: Composite with 6 wt.% Al<sub>2</sub>O<sub>3</sub>



**Figure 15.** Flexural stress-strain curves of EP-Al<sub>2</sub>O<sub>3</sub> nanocomposites

Note: P.E.: Pure Epoxy, C1: Composite with 1 wt.% Al<sub>2</sub>O<sub>3</sub>, C2: Composite with 2 wt.% Al<sub>2</sub>O<sub>3</sub>, C4: Composite with 4 wt.% Al<sub>2</sub>O<sub>3</sub>, C6: Composite with 6 wt.% Al<sub>2</sub>O<sub>3</sub>

This increase is due to the presence of stiff and strong

alumina nanoparticles within the epoxy, which limit the mobility of polymer chains under an exerted load, in addition to their resistance to deformation. However, with an increase in filler content over 2 wt.%, the aggregation of Al<sub>2</sub>O<sub>3</sub> increases; this explains the deterioration of properties after this ratio. This is obvious from the SEM images presented in the current study.

The highest flexural strength was 51.6 MPa at 2 wt.% of Al<sub>2</sub>O<sub>3</sub>, with a 12% increase compared with pure epoxy. This value is lower than that of 135.22 MPa mentioned in the research by Abebe et al. [26], who integrated glass-wool fibers with Al<sub>2</sub>O<sub>3</sub> nanoparticles (hybrid system) to strengthen the polymer, which gives superior mechanical performance.

Table 3 shows the flexural test results for different concentrations of Al<sub>2</sub>O<sub>3</sub>.

The flexural stress and strain were calculated from these equations:

$$\sigma_F = \frac{3PL}{2WB^2} \quad (1)$$

$$\epsilon_F = \frac{6DB}{L^2} \quad (2)$$

where,

- $\sigma_F$  = flexural stress (MPa)
- $\epsilon_F$  = flexural strain
- $P$  = load (N)
- $D$  = deflection (mm)
- $L$  = length span (90 mm)
- $B$  = thickness (5 mm)
- $W$  = width (12.7 mm)

**Table 3.** Flexural test results of EP-Al<sub>2</sub>O<sub>3</sub> nanocomposites

Sample's Code	Composition	Flexural Stress (MPa)	Flexural Strain(%)
P.E.	Pure epoxy	46.00	5.00
C1	99 wt.% epoxy + 1 wt.% Al <sub>2</sub> O <sub>3</sub>	47.73	4.50
C2	98 wt.% epoxy + 2 wt.% Al <sub>2</sub> O <sub>3</sub>	51.60	4.07
C4	96 wt.% epoxy + 4 wt.% Al <sub>2</sub> O <sub>3</sub>	42.14	3.03
C6	94 wt.% epoxy + 6 wt.% Al <sub>2</sub> O <sub>3</sub>	38.27	2.88

### 5.3 Impact properties of Al<sub>2</sub>O<sub>3</sub>-epoxy nanocomposites

The addition of alumina nanoparticles demonstrates an enhancement in the impact properties of the nanocomposites. Figure 16 shows that the impact strength is directly proportional to nano-Al<sub>2</sub>O<sub>3</sub> content.

For EP/Al<sub>2</sub>O<sub>3</sub> nanocomposites, the impact strength peaked at a maximum of 42.52 kJ/m<sup>2</sup> at a concentration of 6 wt.% Al<sub>2</sub>O<sub>3</sub>, improved by about 38.64% compared with a pure epoxy.

This result, which is higher than the 13.34 kJ/m<sup>2</sup> reported by Farhan and Hussein [27], may be due to our use of nanoparticles instead of the microparticles used by the researcher in his study, due to their higher surface area to volume ratio, which provides excellent mechanical properties.

This increase in impact resistance, due to the inhibition of

crack growth by the composite material and the resulting dislocations, leads to a change in crack direction and shape; consequently, the cracks become micro-cracks. This change in crack behavior and the loss of crack energy lead to increased toughness [27].

The impact strength is determined with the following equation:

$$\text{Impact Strength} = U_c / A \quad (3)$$

where,

- $U_c$ : represents fracture impact energy, which is obtained from the Izod impact test instrument in Joules.
- $A$ : is the sample's cross-sectional area in meters.

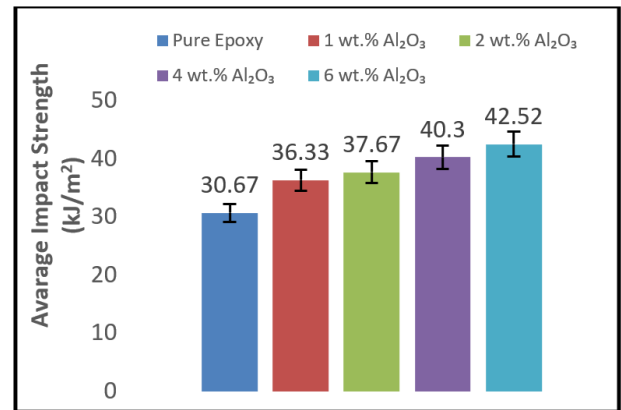


**Figure 16.** Impact strength of EP-Al<sub>2</sub>O<sub>3</sub> nanocomposites  
Note: Error bars show the standard deviation, and each bar shows the mean value of three samples

### 5.4 Hardness properties of Al<sub>2</sub>O<sub>3</sub>- epoxy nanocomposites

The hardness test was conducted on both pure epoxy and nanocomposites at various wt.% of nanoparticles. The Shore D hardness values were measured and graphed in relation to the wt.% of Al<sub>2</sub>O<sub>3</sub>. Figure 17 shows the influence of the weight percentage of nanoparticles on the hardness, where the hardness increased as nanoparticle wt.% increased.

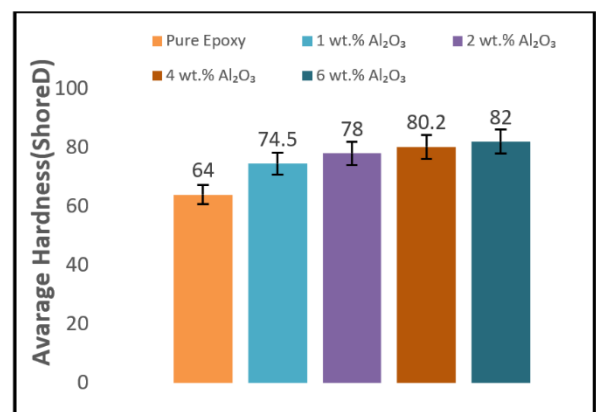


**Figure 17.** Hardness of EP-Al<sub>2</sub>O<sub>3</sub> nanocomposites.  
Note: Error bars show the standard deviation, and each bar shows the mean value of three samples

Our hardness results reached a maximum of 82 Shore D at a ratio of 6 wt.% of Al<sub>2</sub>O<sub>3</sub>, exceeding the value of 73.5 Shore D reported in a research by Al-Mansoori et al. [28]. This is attributed to the increased nanoparticle concentration.

The increased hardness of the nanocomposites is due to the fact that they depend on the bonds between the epoxy resin molecules and the Al<sub>2</sub>O<sub>3</sub> nanoparticles. Increasing the content of Al<sub>2</sub>O<sub>3</sub> nanoparticles reduces the distance between the molecules and improves the adhesion strength, thus making the nanocomposites resistant to penetration and scratching [29].

### 5.5 Fourier Transform Infrared analysis

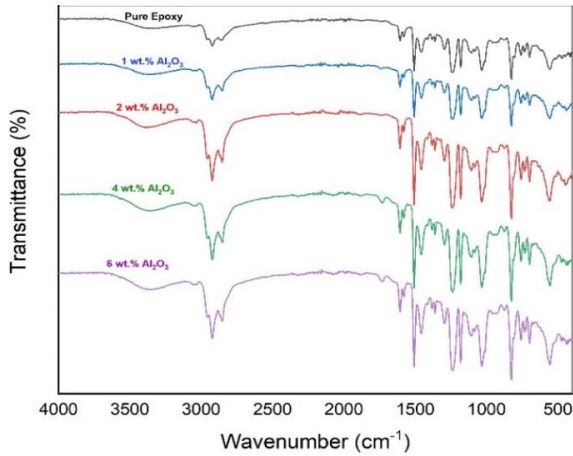


**Figure 18.** Fourier Transform Infrared (FTIR) of EP-Al<sub>2</sub>O<sub>3</sub> nanocomposites

FTIR spectra of epoxy and epoxy nanocomposites are shown in Figure 18. Different functional groups are noticed from the graph. A broad peak at 1106 cm<sup>-1</sup> refers to vibrations

of C-O bonds of epoxide groups (C-O-C).

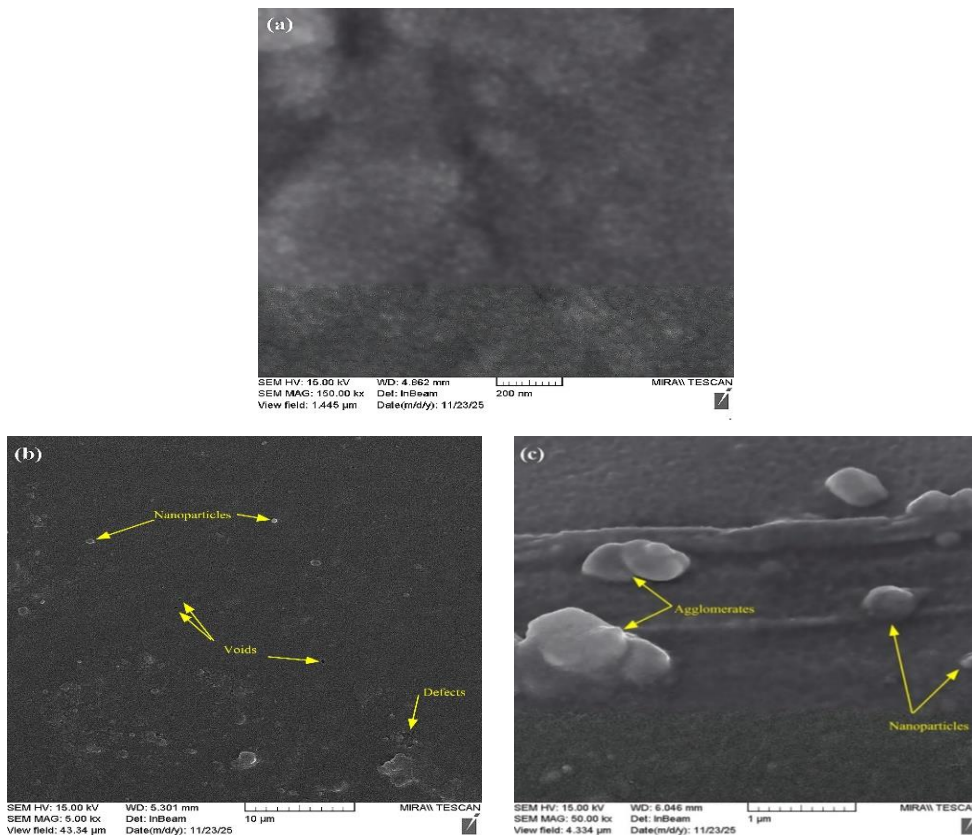
A wide peak at 2922 cm<sup>-1</sup> corresponds to C-H groups, while the weak peak at 1606 cm<sup>-1</sup> indicates vibrations of -OH groups on the surfaces of nano-Al<sub>2</sub>O<sub>3</sub>. A weak band at 1361 cm<sup>-1</sup> conformed with the vibrations of Al-O bonds. The large, wide range in the area of 555-826 cm<sup>-1</sup> is because of Al-O-Al bond vibrations.

These changes help us understand how the nanoparticles affect the way epoxy molecules bond together. Differences in the vibration structures of epoxy molecules have also been noticed. This provides us with more details on how the nanoparticles could change the way the epoxy is arranged.

### 5.6 Microstructural evaluation

The distribution of aluminum oxide nanoparticles (Al<sub>2</sub>O<sub>3</sub>) within the epoxy matrix is an essential factor influencing its mechanical behavior. SEM is necessary to evaluate the distribution of nano-Al<sub>2</sub>O<sub>3</sub> in epoxy. Figure 19 illustrates the surface microstructure of epoxy/alumina nanocomposites, where we observed that the surface of pure epoxy is smooth. In contrast, the incorporation of nano-alumina increases the surface roughness.

The reinforcement shows a homogeneous distribution within the matrix; furthermore, there is strong interfacial adhesion between the reinforcement and the matrix at a ratio of 2 wt.% Al<sub>2</sub>O<sub>3</sub>, (see Figure 19(c)). This uniform distribution reduces stress concentration and thus improves the efficiency of load transfer from the epoxy to the alumina nanoparticles, and this phenomenon explains the enhancement in tensile and flexural properties at this concentration.



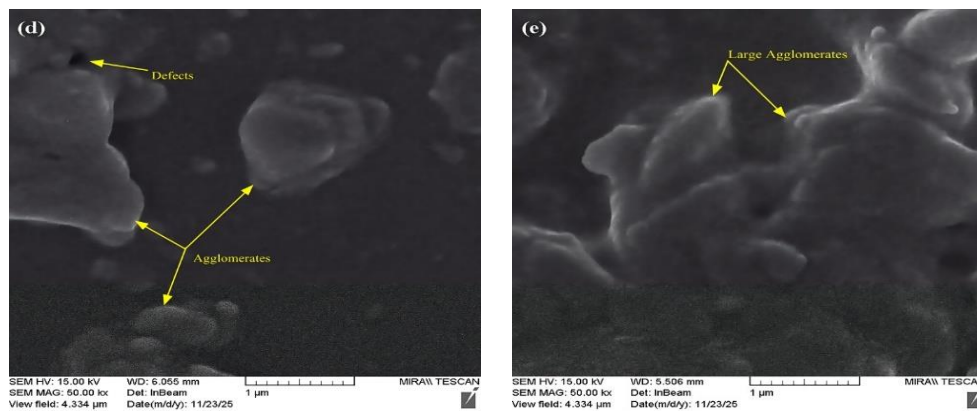


**Figure 19.** Scanning electron microscopy (SEM) images of the surface of epoxy nanocomposites (a) Pure epoxy; (b) 1 wt.% Nano- $\text{Al}_2\text{O}_3$ ; (c) 2 wt.% Nano- $\text{Al}_2\text{O}_3$ ; (d) 4 wt.% Nano- $\text{Al}_2\text{O}_3$ ; (e) 6 wt.% Nano- $\text{Al}_2\text{O}_3$

With an increase in alumina concentration above 2 wt.%, an increase in agglomerations was noticed; these agglomerations act as a stress concentration, leading to crack initiation and propagation, which leads to the deterioration of flexural and tensile properties of the nanocomposites. On the other hand, the surface hardness and impact resistance increase due to the presence of hard alumina nanoparticles, which increase the surface's resistance to scratching, penetration, and fracture. This behavior justifies increases in impact and hardness values up to 6 wt.%, as shown in Figures 19(d) and (e).

## 6. CONCLUSIONS

This investigation shows that adding aluminum oxide nanoparticles to an epoxy matrix significantly enhances its mechanical properties, even if the optimal filler loading depends on the use. The findings indicate that tensile and flexural strengths reach their maximum at a 2 wt.% loading ratio, subsequently decreasing slightly due to localized stress concentrations. Conversely, Shore D hardness and impact resistance continued to improve up to 6 wt.% loading. This indicates that the material can absorb substantial energy and resist surface deformation.

The main result is a synergistic strengthening process in which the nanoparticles restrict the movement of polymer chains and help stabilize cracks. A loading ratio of 2 wt.% is optimal for rigid structures, whereas a loading ratio of 6 wt.% is best for uses that need improved impact and abrasion resistance. To achieve a uniform interface that is necessary for industrial applications, it is best to use ultrasonic dispersion and a regulated curing cycle.

This study concentrates on static mechanical properties at ambient conditions, representing a notable constraint. It is necessary to do additional studies to identify the durability and stress resistance of these nanocomposites. Future studies should focus on investigating the material's dynamic mechanical properties and improving the fillers' surface properties to reduce clustering at higher weight ratios.

## REFERENCES

[1] Upadhyay, A.K., Goyat, M.S. (2024). A review on improved physical and thermal properties of oxide nanoparticles reinforced epoxy composites. *Zastita*

- Materijala, 65(1): 126-142. <https://doi.org/10.62638/ZasMat1038>
- [2] Campbell, F.C. (2010). *Structural Composite Materials*. ASM International. <https://doi.org/10.31399/asm.tb.scm.9781627083140>
- [3] Mohammed, M., Oleiwi, J.K., Mohammed, A.M., Jawad, A.J.A.M., et al. (2023). Comprehensive insights on mechanical attributes of natural-synthetic fibres in polymer composites. *Journal of Materials Research and Technology*, 25: 4960-4988. <https://doi.org/10.1016/j.jmrt.2023.06.148>
- [4] Ali, H., Ali, S., Ali, K., Ullah, S., Ismail, P.M., Humayun, M., Zeng, C. (2025). Impact of the nanoparticle incorporation in enhancing mechanical properties of polymers. *Results in Engineering*, 27: 106151. <https://doi.org/10.1016/j.rineng.2025.106151>
- [5] Kılınçel, M., Kabakçı, G., Tezel, G.B. (2024). Thermo-mechanical behaviours investigation of Nano-Sized  $\text{Al}_2\text{O}_3$ ,  $\text{TiO}_2$ , and Graphene Nanoplatelet Reinforced Epoxy Composites. *Duzce University Journal of Science and Technology*, 12(2): 1201-1216. <https://doi.org/10.29130/dubited.1422620>
- [6] Verma, V., Sayyed, A.H.M., Sharma, C., Shukla, D.K. (2020). Tensile and fracture properties of epoxy alumina composite: Role of particle size and morphology. *Journal of Polymer Research*, 27(12): 388. <https://doi.org/10.1007/s10965-020-02359-z>
- [7] Rusu, M., Sofian, N., Rusu, D. (2001). Mechanical and thermal properties of zinc powder filled high density polyethylene composites. *Polymer Testing*, 20(4): 409-417. [https://doi.org/10.1016/S0142-9418\(00\)00051-9](https://doi.org/10.1016/S0142-9418(00)00051-9)
- [8] Zheng, J., Ozisik, R., Siegel, R.W. (2005). Disruption of self-assembly and altered mechanical behavior in polyurethane/zinc oxide nanocomposites. *Polymer*, 46(24): 10873-10882. <https://doi.org/10.1016/j.polymer.2005.08.082>
- [9] Bagheri, R., Pearson, R.A. (2000). Role of particle cavitation in rubber-toughened epoxies: II. Inter-particle distance. *Polymer*, 41(1): 269-276. [https://doi.org/10.1016/S0032-3861\(99\)00126-3](https://doi.org/10.1016/S0032-3861(99)00126-3)
- [10] Shukla, D.K., Parameswaran, V. (2007). Epoxy composites with 200 nm thick alumina platelets as reinforcements. *Journal of Materials Science*, 42(15): 5964-5972. <https://doi.org/10.1007/s10853-006-1110-8>
- [11] Bello, S.A., Agunsoye, J.O., Hassan, S.E.A., Kana, M.G.Z., Raheem, I. (2015). Epoxy resin based

- composites, mechanical and tribological properties: A review. *Tribology in Industry*, 37(4): 500-524.
- [12] Yang, J., Hasell, T., Wang, W., Howdle, S.M. (2008). A novel synthetic route to metal–polymer nanocomposites by in situ suspension and bulk polymerizations. *European Polymer Journal*, 44(5): 1331-1336. <https://doi.org/10.1016/j.eurpolymj.2008.01.044>
- [13] Fuseini, M., Zaghoul, M.M.Y., Abakar, D., Zaghoul, M.M.Y. (2025). Review of epoxy nano-filled hybrid nanocomposite coatings for tribological applications. *FlatChem*, 49: 100768. <https://doi.org/10.1016/j.flatc.2024.100768>
- [14] Abdalla, M., Dean, D., Robinson, P., Nyairo, E. (2008). Cure behavior of epoxy/MWCNT nanocomposites: The effect of nanotube surface modification. *Polymer*, 49(15): 3310-3317. <https://doi.org/10.1016/j.polymer.2008.05.016>
- [15] Karnati, S.R., Agbo, P., Zhang, L. (2020). Applications of silica nanoparticles in glass/carbon fiber-reinforced epoxy nanocomposite. *Composites Communications*, 17: 32-41. <https://doi.org/10.1016/j.coco.2019.11.003>
- [16] Bharadwaja, K., Srinivasa Rao, S., Babu Rao, T., Pydi, H.P. (2023). Evaluation of mechanical properties for epoxy resin in nano composite diffusion. *Advances in Materials Science and Engineering*, 2023(1): 8598585. <https://doi.org/10.1155/2023/8598585>
- [17] Bittmann, B., Hauptert, F., Schlarb, A.K. (2009). Ultrasonic dispersion of inorganic nanoparticles in epoxy resin. *Ultrasonics Sonochemistry*, 16(5): 622-628. <https://doi.org/10.1016/j.ultsonch.2009.01.006>
- [18] Frigione, M., Lettieri, M. (2020). Recent advances and trends of nanofilled/nanostructured epoxies. *Materials*, 13(15): 3415. <https://doi.org/10.3390/ma13153415>
- [19] Wu, M.J., Lu, L.F., Yu, L.H., Yu, X.Y., Naito, K., Qu, X.W., Zhang, Q.X. (2020). Preparation and characterization of epoxy/alumina nanocomposites. *Journal of Nanoscience and Nanotechnology*, 20(5): 2964-2970. <https://doi.org/10.1166/jnn.2020.17460>
- [20] Zhang, T., Chao, X.J., Liang, J.H., Wang, B., Sun, M.M. (2025). Enhanced mechanical properties of epoxy composites reinforced with silane-modified Al<sub>2</sub>O<sub>3</sub> nanoparticles: An experimental study. *Journal of Composites Science*, 9(5): 252. <https://doi.org/10.3390/jcs9050252>
- [21] Kumar, K., Ghosh, P.K., Kumar, A. (2016). Improving mechanical and thermal properties of TiO<sub>2</sub>-epoxy nanocomposite. *Composites Part B: Engineering*, 97: 353-360. <https://doi.org/10.1016/j.compositesb.2016.04.080>
- [22] Saba, N., Jawaid, M., Sultan, M.T.H. (2019). An overview of mechanical and physical testing of composite materials. In *Mechanical and Physical Testing of Biocomposites, Fibre-Reinforced Composites and Hybrid Composites*, pp. 1-12. <https://doi.org/10.1016/B978-0-08-102292-4.00001-1>
- [23] Abidin, N.M.Z., Sultan, M.T.H., Shah, A.U.M., Safri, S.N.A. (2019). Charpy and Izod impact properties of natural fibre composites. *IOP Conference Series: Materials Science and Engineering*, 670(1): 012031. <https://doi.org/10.1088/1757-899X/670/1/012031>
- [24] Lin, F. (2006). Preparation and characterization of polymer TiO<sub>2</sub> nanocomposites via in-situ polymerization. Master's thesis, University of Waterloo, Canada. <https://www.collectionscanada.gc.ca/obj/s4/f2/dsk3/OWTU/TC-OWTU-920.pdf>
- [25] Lu, K. (2012). *Nanoparticulate Materials: Synthesis, Characterization, and Processing*. John Wiley & Sons. <https://doi.org/10.1002/9781118408995>
- [26] Abebe, Y., Palani, S., Sirahbizu, B. (2025). Effect of Al<sub>2</sub>O<sub>3</sub> nanoparticle on mechanical properties of polyester/glass-wool fiber reinforced polymer composites. *Hybrid Advances*, 10: 100472. <https://doi.org/10.1016/j.hybadv.2025.100472>
- [27] Farhan, A.J., Hussein, W.A. (2020). Effect of alumina contents on the some mechanical properties of alumina (Al<sub>2</sub>O<sub>3</sub>) reinforced polymer composites. *NeuroQuantology*, 18(5): 35-42. <https://doi.org/10.14704/nq.2020.18.5.NQ20165>
- [28] Al-Mansoori, R.O., Diwan, A.A., Taher, A.A. (2021). Influence of alumina and zinc oxidenanoparticles on the tensile, impact and hardness properties of epoxy nanocomposites. *Journal of Physics: Conference Series*, 1973(1): 012047. <https://doi.org/10.1088/1742-6596/1973/1/012047>
- [29] Fouly, A., Alkalla, M.G. (2020). Effect of low nanosized alumina loading fraction on the physicomechanical and tribological behavior of epoxy. *Tribology International*, 152: 106550. <https://doi.org/10.1016/j.triboint.2020.106550>

## NOMENCLATURE

A	Cross-sectional area (m)
B	Thickness (mm)
D	Deflection (mm)
L	Length (mm)
P	Load (N)
U <sub>c</sub>	Fracture impact energy (J)
W	Width (mm)

## Greek symbols

$\sigma_F$	Flexural stress (MPa)
$\epsilon_F$	Flexural strain (%)